A (Near) Zero-cost and Universal Method to Combat Multipaths for RFID Sensing

Ge Wang [†‡], Chen Qian [‡], Kaiyan Cui [†], Han Ding [†], Haofan Cai [‡], Wei Xi[†], Jinsong Han [*♯], Jizhong Zhao [†]
[†]*Xi'an Jiaotong University, Xi'an, China.*
[‡] *University of California, Santa Cruz, CA, USA.*
[*]*School of Cyber Science and Technology, Zhejiang University, China.*
[♯]*Alibaba-Zhejiang University Joint Research Institute of Frontier Technologies, China.*

***Abstract*—There have been increasing interests in exploring the sensing capabilities of RFID to enable numerous IoT applications, including object localization, trajectory tracking, and human behavior sensing. However, most existing methods rely on the signal measurement either in a low multipath environment, which is unlikely to exist in many practical situations, or with special devices, which increase the operating cost.**

This paper investigates the possibility of measuring 'multi-path-free' signal information in multipath-prevalent environments simply using a commodity RFID reader. The proposed solution, Clean Physical Information Extraction (CPIX), is universal, accurate, and compatible to standard protocols and devices. CPIX improves RFID sensing quality with near zero cost – it requires no extra device. We implement CPIX and evaluate its effectiveness on improving the performance on tag localization. The results show that CPIX reduces the localization error by 30% to 50% and achieves the MOST accurate localization by commodity readers compared to existing work.

***Index Terms*—RFID, Sensing, Multipath, Localization**

I. Introduction

As a cost- and energy-efficient solution for the Internet of Things (IoT), Radio Frequency IDentification (RFID) technology has been widely used to connect tagged objects in ubiquitous applications, such as retailing, warehouse, transportation, manufactures, and human-behavior sensing [1]–[6]. Besides its basic tag-identification function, there has been a growing interest in recent research to discover the sensing capability of RFID tags that reflects the spatial-temporal information of the tags in the physical world. Typical applications of RFID sensing include localization, trajectory tracking, human behavior sensing, *etc.*. The majority of these applications rely on the measurement of the received signal data from tags, specifically, the *phase shift* between the reader to tags (we use "*phase*" hereafter).

For RFID sensing applications, the 'multipath-free' phase measurement of the backscatter signals is a must for their correct operations. The multipath-free phase is defined as the phase without environment affection from a tag to the reader, which can reflect the actual distance and relative location changes. In this paper, we call the line-of-sight (LOS) signal phase as the *clean phase*. Unfortunately, in most practical RFID setups, signals may be reflected by various reflectors in the environment [13], including walls, furniture, shelves, and moving persons. We consider these environments as *multipath-prevalent* environments. Multiple reflected signals combine with each other and result in measurement results extremely different from the clean ones. Recent localization methods *either cannot combat multipaths or require extra devices/restrictions.* They might assume low-multipath environments, no moving persons [7], or apply the following two approaches: 1) Collecting plenties of training data in the deployment area to estimate the multipath [12], [17]. This type of methods only considers the static reflectors but obviously does not work when moving persons exist. 2) Using special hardware including Software Defined Radio (SDR) [10], [11], synchronised antenna array (*e.g.* MUSIC algorithm), moving antennas [12], [13], robots [8], [12], and broadband nonlinear backscatter devices [9]. These methods increase the device cost, may not be compatible with existing RFID systems, and only work for certain specific applications. We specify them in Sec. II.

This paper presents a low-cost, universal, and accurate solution of Clean Physical Information eXtraction (CPIX) in multipath prevalent environments. CPIX **achieves a significant quality gain of RFID sensing with little cost** – it requires no extra device or restriction in addition to the current operating RFID systems: reader, tags, and a data analysis server. Hence it is **a simple yet fundamental improvement** to a diverse group of RFID sensing applications.

We resolve a number of challenges in the design and implementation of CPIX, including the uncontrollable and unpredictable multipath reflections and device diversity. The basic idea of CPIX is to conduct signal measurement from multiple channels of a commodity reader. Our unique innovation is that we decompose the measured data into two parts: the contribution determined by the LOS signal and the contribution by the reflected signals, and then derive their mathematical relationships.

Our contributions are summarized as follows.

1) CPIX is the first generalized solution that can measure the multipath-free physical information by only COTS

This work was partially supported by the National Key R&D Program of China 2017YFB1003000, National Natural Science Foundation of China Grant No. 61832008, 61802299, 61872285, 61772413, Fundamental Research Funds for the Central Universities, and the Research Institute of Cyberspace Governance in Zhejiang University. Chen Qian and Haofan Cai were partially supported by National Science Foundation Grants 1717948 and 1750704.

978-1-7281-2700-2/19/$31.00 2019 © IEEE

RFID devices. It is a middleware program running on the back server without extra hardware or hardware modification.
2) CPIX needs no deployment of reference/anchor tags or sensors, nor training data collection. It highly improves the application variety and convenience of CPIX.

The rest of paper is organized as follows. We review the related work in Section II. The model and validation of multipath reflections are presented in Section III. The system design and evaluation can be found in Section IV and V. Finally we conclude this paper in Section VI.

II. Related Work

Tag localization and trajectory tracking: Due to the close relationship with the travel distance of signals, phases have been widely used in tag trajectory tracking and localization. The accuracy of most localization [7] methods heavily rely on a low-multipath environment. BNB [9], RFind [11] and TurboTrack [8] are recent localization methods that can combat the multipath effect. However, they both require extra hardware such as software-defined radio, non-commodity readers, antenna arrays and even self-defined tags.

LOS identification techniques: Prior work in other technologies, such as WiFi and 60GHz wireless, may employ a frequency domain transform method to identify the line-of-sight signals [11]. The basic idea is to transform the frequency domain signals in a certain bandwidth into a time domain. However, this method cannot be applied in COTS RFID system. That is because commercial RFID devices transmit RF signals at a certain central frequency and the bandwidth is extremely small (about 4MHz with InpinJ R420). Besides frequency domain transformation, MUSIC is an algorithm used for finding the emitters' locations. However, the COTS RFID systems do not support the synchronous antenna array, even if it equipped with an antenna hub [15].

III. Background

A passive RFID tag communicates with the RFID reader by backscattering its electric signals. Since there are prevalent reflectors in the real world, the received signals at the reader's antenna can be expressed as a superposition of the line-of-sight (LOS) signal P_L and the combined multipath signals P_M, *i.e.*:

$$P(\rho,\beta) = \underbrace{\rho_L \cdot \cos(2\pi f \cdot t_L + \theta)}_{LOS\ signal\ P_L} + \underbrace{\rho_M \cdot \cos(2\pi f \cdot t_M + \alpha)}_{Multipath\ signal\ P_M} \tag{1}$$

where f denotes the signal frequency, which can be considered as identical for both LOS and multipath signals. t_L and t_M are the signal transmitting time of LOS signal and multipath ones, respectively. β, θ and α represent the phases of the received signal, LOS signal and combined multipath signals respectively. And ρ, ρ_L and ρ_M are signals' amplitudes.

Observing the aforementioned elaborations, we find that the received signal P is not a linear relationship with the LOS signal P_L. In other words, the physical data we measured from the received signal cannot accurately reflect the exact values

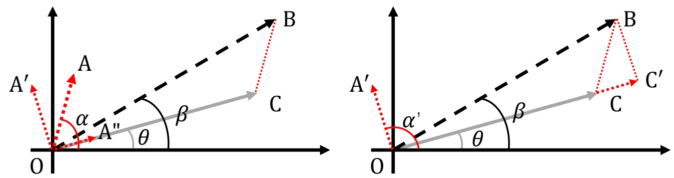

(a) Signals superposition (b) Decompose signals

Fig. 1. Relationships between β and θ

and changes of the LOS signal, causing existing work to be error-prone in multipath-prevalent environments.

IV. CPIX Design

CPIX can be separated into three steps, including **1)** Phase decomposition. **2)** Clean phase calculation. **3)** RSS calculation.

A. Phase decomposition

As aforementioned, the received signal is a vector superposition of the LOS signal and other reflected ones. Therefore, in this step, we first explore the relationship between the LOS signal P_L and the received signals P.

We illustrate the relationship between the measured phase β and the clean phase θ, in Fig. 1. The radius of the vector represents the amplitude of the signal and the polar angle represents the current phase. As shown in Fig. 1(a), the gray line $\overrightarrow{OC}$ denotes the line-of-sight signal P_L, while the red line $\overrightarrow{OA}$ represents the superposition of all reflected signals, *i.e.*, P_M. Their phases are θ and α, respectively. We first build a bridge between the multipath signal and LOS signal. As shown in Fig. 1(a), we decompose the multipath vector $\overrightarrow{OA}$ into two parts, one vector $\overrightarrow{OA'}$ is perpendicular to LOS signal $\overrightarrow{OC}$, while another vector $\overrightarrow{OA''}$ is parallel to $\overrightarrow{OC}$. We find that θ and new α' do not have a linear relationship with the phase β. In order to process them in a mathematical way, we define two *scalars*, $\hat{\theta}$ and $\hat{\alpha}$, whose sum is the received phase β, *i.e.*,

$$\beta = \hat{\theta} + \hat{\alpha} \tag{2}$$

where the two variables, $\hat{\alpha}$ and $\hat{\theta}$, have the following relationship with θ:

$$\begin{cases} \hat{\theta} = (\theta + \hat{k} \cdot \pi)\ mod\ 2\pi, where\ \hat{k} \in Z \\ \hat{\alpha} = \arctan(-1)^{k_0} \cdot \frac{|\overrightarrow{OC'}|}{|\overrightarrow{OA'}|}, \end{cases} \tag{3}$$

In this way, we transform the measured phase β from the superposition of two unknown phases into a simple sum of two scalar phases $\hat{\alpha}$ and $\hat{\theta}$. In the following section, we will elaborate on how to calculate the value of the image phase $\hat{\theta}$ and finally infer the value of the clean phase θ.

B. Clean phase calculation

In this section, we try to calculate the exact value of the *mirror image phase* $\hat{\theta}$ by exploring the internal relationship among the measured phases β in multiple channels. According our observation in numerous experiments, we have a conjecture about the received phase β in multiple channels.

$$\beta_n = \hat{\alpha_n} + \hat{\theta} + (n-1) \cdot \Delta\hat{\theta} \tag{4}$$

where β_n is the received phase in channel n. $\hat{\theta}$ refers to the mirror image phase in the first channel. $\hat{\alpha_n}$ is the *multipath variable* in channel n. To validate the aforementioned conjecture, we perform a set of experiments. We place a tag in two different places, *i.e.*, an open area and a multipath-prevalent environment, and record the reported phases β_n in each channel. The results are shown in Fig. 2(a). The measurement phases in the open area are roughly on a straight line y'. That is because the effect of multipath signals in the open area is negligible when it is compared with the line-of-sight one, *i.e.*, $\hat{\alpha_n} \ll \Delta\hat{\theta}$. Hence we can safely express the straight line y' as:

$$y' = \kappa' \cdot n + d', where\ \kappa' = \Delta\hat{\theta}, d' = \hat{\theta} - \Delta\hat{\theta} \tag{5}$$

We call y' as the ideal line, which is only correct when there is no multipath effect. On the other hand, in a narrow space, the multipath effect becomes severe. In the second experiment, the multipath variables $\hat{\alpha_n}$ cannot be ignored. Under this circumstance, we fit these reported phases β_n in all channels into a line. We define the fitting line as $y_n = \kappa \cdot n + d$, which has the minimal φ as follows:

$$\varphi = \sum_{n=1}^{N} \omega_n \cdot (y_n - \beta_n)^2, \tag{6}$$

where ω_n is the weight of channel n. We define the weight function to reduce the influence of outliers. To retrieve the exact value of tag's mirror image phase $\hat{\theta}$, we analogize the Eq. 4 as a matrix equation $A \cdot x = b$, *i.e.*,

$$A_{N\times(N+2)} = \begin{bmatrix} 1 & 0 & 0 & ... & 0 & 1 & 0 \\ 0 & 1 & 0 & ... & 0 & 1 & 1 \\ 0 & 0 & 1 & ... & 0 & 1 & 2 \\ . & . & . & . & . & . & . \\ . & . & . & . & . & . & . \\ . & . & . & . & . & . & . \\ 0 & 0 & 0 & ... & 1 & 1 & N-1 \end{bmatrix}, \tag{7}$$
$$x^T_{N+2\times 1} = [\hat{\alpha}_1, \hat{\alpha}_2, \hat{\alpha}_3, ...\hat{\alpha}_N, \hat{\theta}, \Delta\hat{\theta}],$$
$$b^T_{N\times 1} = [\beta_1, \beta_2, \beta_3, ...\beta_N],$$

where $A_{N\times(N+2)}$ is the coefficients matrix, $x_{(N+2)\times 1}$ is the unknown variable matrix, and $b_{N\times 1}$ represents the matrix of reported phases. And $(\cdot)^T$ represents the transpose of the matrix. Obviously, Eq. 7 is a set of non-homogeneous linear equations. Since we have $N + 2$ unknown variables and N equations, the solution of x has infinite possible candidates. To find out the valid solution of x, we need to establish two more additional equations.

Equation I: Intuitively, the first equation we built is based on the fitting line:

$$\kappa = \Delta\hat{\theta} + e_1,\ e_1 = \frac{N \cdot \sum \omega \cdot n \cdot \hat{\alpha}_n - \sum \omega \cdot n \cdot \sum \omega \cdot \hat{\alpha}_n}{N \cdot \sum \omega \cdot n^2 - (\sum \omega \cdot n)^2}. \tag{8}$$

Equation II: As shown in Fig. 2(b), the points y_n on the fitting line have a gap with the reported phase β_n. We define the difference between each pair of y_n and β_n as *residual error* S_n. The residual error S_n can be transformed into another expression, *i.e.*, the second desired equation:

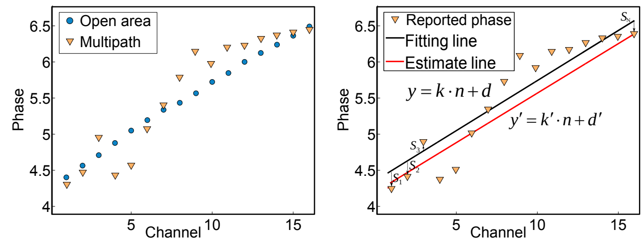

(a) The reported phases (b) The fitting line

Fig. 2. The reported phases in 16 channels

$$S_n = n \cdot e_1 + e_2 - \hat{\alpha}_n, n = 1, 2, 3...N$$
$$where\ e_2 = \frac{\sum \omega \cdot n^2 \cdot \sum \omega \cdot \hat{\alpha}_n - \sum \omega \cdot n \cdot \hat{\alpha}_n \cdot \sum \omega \cdot n}{N \cdot \sum \omega \cdot n^2 - (\sum \omega \cdot n)^2}, \tag{9}$$

With Eq. 8 and 9, we can solve all the unknown variables in matrix x, including the mirror image phase $\hat{\theta}$ and the multipath variable $\hat{\alpha}$. Since $\hat{\theta} = (\theta + \hat{k} \cdot \pi)\ mod\ 2\pi$ (Eq. 3), the clean phase θ has two feasible solutions. However, the value of clean phase θ is limited by the received phase β: $\angle BOC' = (\theta - \beta)\ mod\ 2\pi < \frac{\pi}{2}$. Hence we can determine the solution of θ that meets such a requirement.

V. Evaluation and Case Study

A. Prototype implementation

The CPIX prototype includes **nothing more than the basic components** of a typical passive RFID system: an RFID reader, several directional antennas, a set of tags, and a backend server, which are all commodity devices. In specific, we use an ImpinJ Speedway R420 RFID reader, four Laird S9028PCL directional antennas, and four types of mainstream UHF passive RFID tags: ImpinJ E41C, E41B and Alien 9710, Alien 9640. The R420 reader operates at the UHF frequency band (920.625 $\sim$ 924.375 MHz) and is able to hop over 16 channels. The gaps between two adjacent channels are the same, *i.e.*, 0.25 MHZ. The ground truth data are obtained by laser range finder and Kinect, which are not required by CPIX.

B. Performance on Tag localization

Localization is the most commonly proposed RFID sensing application. It is also the basis of another important application, trajectory tracking. To emulate the practical environments, we conduct experiments in three different environments, *i.e.*, the "*hallway*" (HW), "*laboratory*" (Lab), and "*Office*" (OF). In the three environments, multipath reflections exist and could be a critical factor that impacts the localization accuracy. We deploy 80 passive RFID tags in all. Among them, 12 are ImpinJ E41C tags, 40 are ImpinJ E41B tags, 20 are ALN-9710 and the other 8 are ALN-9640 tags, for the reader to localize. We utilize four antennas and form them as a square. The coordinate origin of the deployment space is set as the center of this square. The tags we try to localize are at different positions. Their location varies

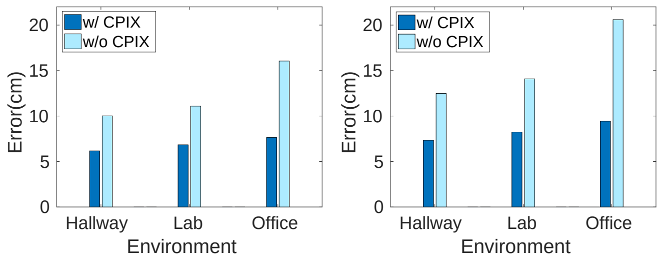

(a) No mobility

(b) With mobility

Fig. 3. Mean localization errors

TABLE I
COMPARISON OF STATE-OF-THE-ART RFID LOCALIZATION SCHEMES.

Localization work	Multipath-prevalent?	Dimension	Median error
RF-IDraw [14]	not allow	Three	19cm
Tagoram [16]	not allow	Two	12.3cm
BackPos [7]	not allow	Two	12.8cm
RFly [10]	allow	Three	19cm
PinIt [13]	allow	Three	11.2cm
CPIX (HW/OF)	allow	Three	6.17/7.63cm

among -82cm∼16cm in height (z-axis), -89cm∼104cm in width (y-axis), and 92cm∼300cm in depth (x-axis). For each environment, we conduct two sets of experiments. One is without moving objects and another has one volunteer keep walking arbitrarily in the area. The walking speed is 1∼2m/s. We call these two setups as "*no mobility*" and "*with mobility*". The localization algorithm is a recently developed Hyperbola-based Localization (HL) method introduced in [7], [14].

Localization errors. In Fig. 3, we show the mean localization errors of the HL algorithm when using the CPIX phase (w/ CPIX) and the phase data from the reader API (w/o CPIX) respectively. We find that CPIX evidently reduces the HL errors in all environments, with and without mobility. The error reduction rate in Hallway is 38.4% (10.02cm to 6.17cm) without mobility and 41.2% (12.48cm to 7.34cm) with mobility. The error reduction rate in Lab is 32.7% (11.09cm to 7.58cm) without mobility and 41.5% (14.09cm to 8.24cm) with mobility. The error reduction rate in Office is 52.5% (16.05cm to 7.63cm) without mobility and 54.2% (20.6cm to 9.43cm) with mobility. We find when the environment is more complex and includes mobility, the multipath are more significant and the error reduction using CPIX is more obvious.

We compare the CPIX-enabled HL with some state-of-art localization schemes, including PinIt [13], RF-IDraw [14], Tagoram [16], BackPos [7], and RFly [10]. We do not include recent work such as Broadband Nonlinear Backscatter [9] and RFind [11] that use self-built (and expensive) devices.

Note for all results in the table, the distance to the reader used in our experiments is no less than the corresponding distance of the results from these existing methods. The localization environments in our experiments are **no better** than other work. CPIX based localization provides the lowest errors in both the median and worst cases. As shown in Tab. I, most of those methods operate with low multipath environments.On the contrary, CPIX based localization does not need any extra hardware deployment or training procedure and works well in multipath-prevalent environments. CPIX based localization achieves **the smallest tag localization error in the literature** for multipath-prevalent environments using COTS RFID devices.

VI. CONCLUSION

In this paper, we present CPIX, the first generalized and low-cost solution to calculate accurate clean physical information for RFID sensing in the practical multipath-prevent environment. We use a new signal analysis model to extract the clean physical information using multi-channel measurement. The experiments indict that CPIX can achieve good accuracies.

REFERENCES

[1] CAI, H., WANG, G., SHI, X., XIE, J., WANG, M., AND QIAN, C. When Tags 'Read' Each Other: Enabling Low-cost and Convenient Tag Mutual Identification. In *Proceedings of IEEE ICNP* (2019).

[2] DING, H., QIAN, C., HAN, J., WANG, G., XI, W., ZHAO, K., AND ZHAO, J. RFIPad: Enabling Cost-efficient and Device-free In-air Handwriting using Passive Tags. In *Proceedings of IEEE ICDCS* (2017).

[3] HAN, J., DING, H., QIAN, C., MA, D., XI, W., WANG, Z., JIANG, Z., AND SHANGGUAN, L. CBID: A customer behavior identification system using passive tags. In *Proceedings of IEEE ICNP* (2014).

[4] HAN, J., QIAN, C., WANG, X., MA, D., ZHAO, J., XI, W., JIANG, Z., AND WANG, Z. Twins: Device-free object tracking using passive tags. *IEEE/ACM Transactions on Networking (TON) 24*, 3 (2016), 1605–1617.

[5] JIN, H., WANG, J., YANG, Z., KUMAR, S., AND HONG, J. WiSh: Towards a Wireless Shape-aware World Using Passive RFIDs. In *Proceedings of ACM MobiSys* (2018).

[6] LI, H., YE, C., AND SAMPLE, A. P. IDSense: A Human Object Interaction Detection System Based on Passive UHF RFID. In *Proceedings of ACM CHI* (2015).

[7] LIU, T., YANG, L., LIN, Q., GUO, Y., AND LIU, Y. Anchor-free backscatter positioning for RFID tags with high accuracy. In *Proceedings of IEEE INFOCOM* (2014).

[8] LUO, Z., ZHANG, Q., MA, Y., SINGH, M., AND ADIB, F. 3D backscatter localization for fine-grained robotics. In *Proceedings of USENIX NSDI* (2019).

[9] MA, Y., HUI, X., AND KAN, E. C. 3D Real-time Indoor Localization via Broadband Nonlinear Backscatter in Passive Devices with Centimeter Precision . In *Proceedings of ACM Mobicom* (2016).

[10] MA, Y., SELBY, N., AND ADIB, F. Drone Relays for Battery-Free Networks. In *Proceedings of ACM SIGCOMM* (2017).

[11] MA, Y., SELBY, N., AND ADIB, F. Minding the billions: Ultra-wideband localization for deployed rfid tags. In *Proceedings of ACM MobiCom* (2017).

[12] SHANGGUAN, L., AND JAMIESON, K. The design and implementation of a mobile RFID tag sorting robot. In *Proceedings of ACM MobiSys* (2016).

[13] WANG, J., AND KATABI, D. Dude, where's my card?: RFID positioning that works with multipath and non-line of sight. In *Proceedings of ACM SIGCOMM* (2013).

[14] WANG, J., VASISHT, D., AND KATABI, D. RF-IDraw: Virtual touch screen in the air using RF signals. In *Proceedings of ACM SIGCOMM* (2014).

[15] WANG, J., XIONG, J., JIANG, H., CHEN, X., AND FANG, D. D-Watch: Embracing "bad " Multipaths for Device-Free Localization with COTS RFID Devices. In *Proceedings of ACM CoNEXT* (2016).

[16] YANG, L., CHEN, Y., LI, X., XIAO, C., LI, M., AND LIU, Y. Tagoram: Real-time tracking of mobile RFID tags to high precision using COTS devices. In *Proceedings of ACM MOBICOM* (2014).

[17] YANG, L., LIN, Q., LI, X., LIU, T., AND LIU, Y. See through walls with COTS RFID system! In *Proceedings of ACM MOBICOM* (2015).